Journal of Anatomy

J. Anat. (2019) **235**, pp803–810 doi: 10.1111/joa.13030

Sulcal pattern variation in extant human endocasts

Edwin J. de Jager,[1] Albert N. van Schoor,[1] Jakobus W. Hoffman,[2] Anna C. Oettlé,[1,3] Caroline Fonta,[4] Muriel Mescam,[4] Laurent Risser[5] and Amélie Beaudet[1,6]

[1]*Department of Anatomy, Faculty of Health Sciences, University of Pretoria, Pretoria, South Africa*
[2]*South African Nuclear Energy Corporation, Pelindaba, South Africa*
[3]*Department of Anatomy and Histology, Sefako Makgatho Health Sciences University, Pretoria, South Africa*
[4]*Centre de Recherche Cerveau et Cognition, Université de Toulouse, UPS, Toulouse, France*
[5]*Institute de mathématiques de Toulouse, Université de Toulouse, UPS, Toulouse, France*
[6]*School of Geography, Archaeology and Environmental Studies, University of the Witwatersrand, Johannesburg, South Africa*

Abstract

Our knowledge of human brain evolution primarily relies on the interpretation of palaeoneurological evidence. In this context, an endocast or replica of the inside of the bony braincase can be used to reconstruct a timeline of cerebral changes that occurred during human evolution, including changes in topographic extension and structural organisation of cortical areas. These changes can be tracked by identifying cerebral imprints, particularly cortical sulci. The description of these crucial landmarks in fossil endocasts is, however, challenging. High-resolution imaging techniques in palaeoneurology offer new opportunities for tracking detailed endocranial neural characteristics. In this study, we use high-resolution imaging techniques to document the variation in extant human endocranial sulcal patterns for subsequent use as a platform for comparison with the fossil record. We selected 20 extant human crania from the Pretoria Bone Collection (University of Pretoria, South Africa), which were detailed using X-ray microtomography at a spatial resolution ranging from 94 to 123 μm (isometric). We used Endex to extract, and Matlab to analyse the cortical imprints on the endocasts. We consistently identified superior, middle and inferior sulci on the frontal lobe; and superior and inferior sulci on the temporal lobe. We were able to label sulci bordering critical functional areas such as Broca's cap. Mapping the sulcal patterns on extant endocasts is a prerequisite for constructing an atlas which can be used for automatic sulci recognition.
Key words: brain cast; cerebral variation; human neuroanatomy; palaeoneurology; sulci detection.

Introduction

Together with comparative anatomy, the endocast or replica of the internal table of the bony braincase can be used to reconstruct the timeline and mode of cerebral changes in human evolution (Holloway, 1978; Holloway et al. 2004; de Sousa & Cunha, 2012). Identifying cerebral imprints in endocasts of fossil hominin specimens is challenging due to poor preservation of fossils and inconsistencies in characterisation and identification of landmarks. Long-standing concerns exist regarding the correlation between the gyral and sulcal patterns on the brain, and the bulges and furrows imprinted on the braincase (Le Gros Clark et al. 1936; Kobayashi et al. 2014; Minh & Hamada, 2017; Bruner & Ogihara, 2018). Controversy also surrounds early descriptions of these patterns in fossil endocasts, which mostly relied on visual inspection and palpation of the endocranial surface (Falk, 1980a,b, 1983; Holloway, 1981). The accuracy of the cerebral details on the endocranial surface is also affected by the presence of intracranial components, including arterial supply of the brain, cerebrospinal fluid and meningeal membranes (Neubauer, 2014). The sulcal patterns in extant human brains are also variable, further complicating anatomical comparisons (Ribas, 2010).

The accurate identification of sulcal imprints on fossil endocasts is of prime interest in palaeoneurology. Despite the uncertainty surrounding the correspondence of cerebral areas delimited by sulci and the functional areas of the brain (Amunts et al. 1999), sulcal variation may reliably predict the location of primary and secondary areas in the brain, such as visual, somatosensory and motor areas (Fischl et al. 2008). The ability to identify sulci in endocasts of fossil hominoids may inform our understanding of evolutionary trends in cortical areas involved in specific functions. For example, the evolution of the visual cortex and the Broca's

Correspondence
Edwin J. De Jager, Department of Anatomy, BMS Building, Prinshof Campus, University of Pretoria, Private Bag X323, Arcadia 0001, South Africa. E: edwin.dejager@tuks.co.za

Ethical clearance was obtained from the Main Research Ethics committee of the Faculty of Health Science, University of Pretoria, August 2017 (No: 339/2017).

Accepted for publication *21 May 2019*
Article published online *17 June 2019*

cap has been intensively discussed in non-human and human fossil hominin taxa (Falk, 1980a,b, 1983, 2014; Holloway, 1981; Carlson et al. 2011; Beaudet, 2017; García-Tabernero et al. 2018; Holloway et al. 2018).

Technological advances in medical imaging techniques have enabled palaeoneurologists to compare anatomical features in more detail. Endocasts of fragmented fossil cranial vaults can be virtually extracted, reconstructed and interpreted without damaging the specimen (Spoor et al. 2000; Gunz et al. 2010; Neubauer et al. 2012, 2018; Neubauer, 2014; Beaudet & Gilissen, 2018). We used high-resolution microtomography to investigate endocranial structural organisation and variation in extant human skulls. This non-invasive, observer-independent approach was recently used to automatically detect sulcal imprints on fossil endocasts (Beaudet et al. 2016a; Beaudet & Gilissen, 2018). These studies identified a need for an atlas of variation in sulcal patterns in extant human crania. This study documents the variation in sulcal pattern on extant human endocasts for subsequent use as a reference in palaeoneurological studies.

Materials and methods

We selected 20 individual, non-pathological adult crania from the Pretoria Bone Collection (University of Pretoria, South Africa) (L'Abbé et al. 2005), consisting of 10 individuals of African and 10 individuals of European ancestry with equal proportions of females and males . The crania were from individuals of known age, ranging from 30 to 80 years old. We scanned the crania using micro X-ray computer tomography at the MIXRAD facility, housed at Necsa, Pelindaba, South Africa, at a spatial resolution ranging from 94 to 123 μm (isometric) (Hoffman & De Beer, 2012).

The endocasts were virtually extracted and reconstructed using ENDEX software (Subsol et al. 2010) (Fig. 1A). Based on previous studies (Subsol et al. 1996, 1998), we detected the cortical relief in endocasts using an algorithm that automatically detects topographical variations in, for example, crest lines on 3D meshes (Yoshizawa et al. 2007, 2008) (Fig. 1C). We manually removed the structures of no interest, for example the imprints formed by the middle meningeal arteries and cranial sutures, by referring to brain atlases (Connolly, 1950; Ono et al. 1990). We manually labelled the detected sulci using a program created with MATLAB R2013a v8.1 (Mathworks) which assigns a label to the selected curves (Beaudet et al. 2016b) (Fig. 1D).

Results

The frequencies of sulci identified on the left (LH) and right (RH) hemispheres of the crania are alphabetically listed in Table 1.

Frontal lobes

We identified impressions of the branches of the orbital sulcus on the orbital surface of all cranial endocasts. We identified a clear transverse orbital sulcus impression on nine crania, resulting in the generally known 'H' or 'Y' pattern. We did not consider the olfactory sulcus in any of the crania due to the distortion caused by the impression from the cribriform plate.

We clearly identified the fronto-orbital sulcus of the frontal lobe (*sensu* Ono et al. 1990) in 75% of LHs and 60% of

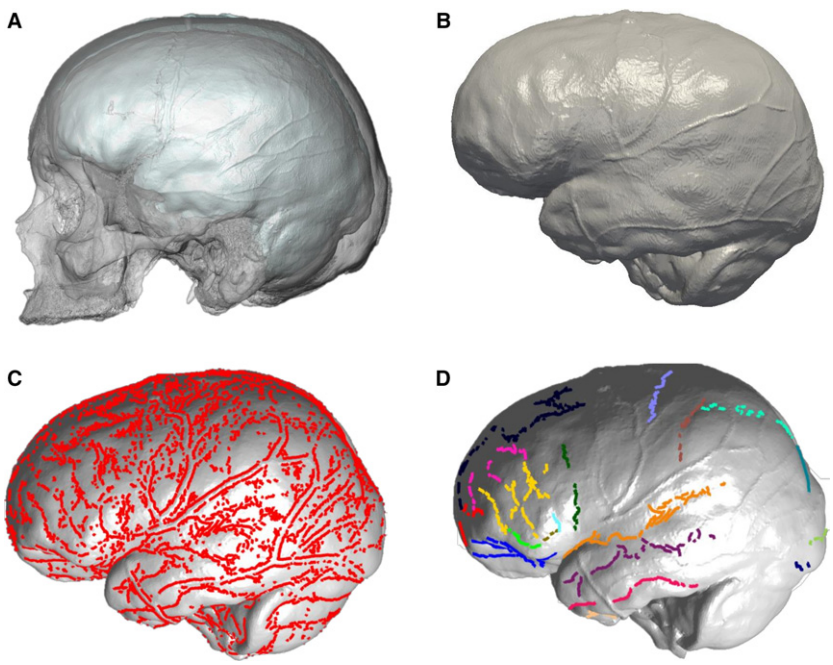

Fig. 1 Automatic extraction of an extant human endocast using ENDEX (A). Resulting endocast mesh (B). Application of crest line detection algorithm (C). Endocast after cleaning of crest lines and labelling (D).

Table 1 Frequency of sulci observed for left and right hemispheres in human

Sulcus	Left	Right
anterior horizontal ramus (*hr*)	40%	20%
ascending ramus (*ar*)	40%	20%
central (*c*)	55%	50%
collateral (*col*)	25%	0%
frontomarginal (*W*)	85%	100%
fronto-orbital (*fo*)	75%	60%
inferior frontal (*if*)	85%	90%
inferior temporal (*it*)	100%	95%
middle frontal (*fm*)	90%	75%
intraparietal (*ip*)	30%	15%
lateral calcarine (*lc*)	55%	20%
inferior/lateral occipital (*oci*)	50%	60%
lunate (*L*)	80%	70%
occipitotemporal (*oct*)	35%	45%
orbital sulci (*o*)	100%	100%
postcentral (*pt*)	20%	15%
precentral (*pc*)	35%	40%
retro-calcarine (*rc*)	20%	10%
rhinal (*rh*)	25%	60%
superior frontal (*sf*)	95%	90%
superior temporal (*st*)	75%	90%
Sylvian fissure (*S*)	95%	85%
transverse occipital (*otc*)	70%	55%

RHs (Figs 2 and 3). We identified the fronto-marginal sulcus in 85% of LHs and in 100% of RHs (Fig. 2H).

We clearly identified the superior frontal sulcus in 95% of LHs and in 90% of RHs. We observed connections between the superior frontal sulcus and the fronto-marginal sulcus ($n = 12$), middle frontal sulcus ($n = 7$) and precentral sulcus ($n = 2$) (Figs 2 and 3).

We identified the middle frontal sulcus in 90% of LHs and in 75% of RHs. We mostly observed a segmental pattern ($n = 13$) (Fig. 3A).

We identified impressions of the inferior frontal sulcus in 85% of LHs and in 90% of RHs. We observed up to seven side branches in one cranium, some of which extended onto the orbital surface and others connecting with the middle frontal sulcus (Fig. 3R). The inferior frontal sulcus was not clearly defined in five crania; which may be due to distortion caused by overlaying blood vessels (Fig. 3F). We could only observe the precentral sulcus in 35% of the LHs and 40% of the RHs (Figs 2 and 3).

We clearly identified the Sylvian fissure in 95% of LHs and 85% of RHs. We could only identify the anterior horizontal ramus and ascending ramus in eight LHs and four RHs (Figs 2 and 3).

Parietal lobes

We identified the central sulcus in 55% of LHs and 50% of the RHs (Fig. 2). We observed the postcentral sulcus in 20% of LHs and 15% of RHs (Fig. 2A).

We identified the intraparietal sulcus on the LH of six crania and on the RH of three crania (Fig. 2A). We identified the transverse occipital sulcus, or posterior branch of the intraparietal sulcus (Ono et al. 1990) in 70% of LHs and 55% of RHs (Fig. 2E,F).

Occipital lobes

We identified the lateral occipital sulcus in 50% of LHs and 60% of RHs as a small sulcus along the most lateral and inferior border of the occipital lobe. We identified fragments of the lunate sulcus in 80% of LHs and 70% of RHs (Figs 2 and 3). We could also identify the lateral calcarine sulcus (LHs = 55%; RHs = 20%) and retro-calcarine sulcus (LHs = 20%; RHs = 10%), medial to the lunate sulcus (Fig. 4).

Temporal lobes

We observed the superior temporal sulcus in 75% of LHs and 90% of RHs, with the anterior segment clearly imprinted. We observed the inferior temporal sulcus in 100% of LHs and 95% of RHs with most crania exhibiting an anterior extension to the temporal pole (Figs 2 and 3).

When observing the basal surface of the temporal lobe, we identified the rhinal sulcus in 25% of LHs and 60% of RHs. The rhinal sulcus is frequently subject to a substantial degree of distortion due to the presence of the middle meningeal artery. We observed similar results for the collateral sulcus (LHs = 25%; RHs = 0%) and the occipitotemporal sulcus (LHs = 35%; RHs = 45%).

Left vs. Right hemisphere

We noted left–right hemisphere asymmetry for the lateral calcarine sulcus (LHs = 55%; RHs = 20%, $P < 0.05$), the rhinal sulcus (LHs = 25%; RHs = 60%, $P < 0.05$) and the collateral sulcus (LHs = 20%; RHs = 0%, $P < 0.05$) (Fig. 5).

Male vs. Female

We did not observe any differences in sulcal patterns between male and female crania ($P > 0.05$). In general, we more readily identified sulci in female (~ 3% more frequent) crania than male crania (Fig. 6). We saw sex differences in the RHs in the impression of the fronto-orbital sulcus (M = 40%; F = 80%), precentral sulcus (M = 50%; F = 30%), transverse occipital sulcus (M = 40%; F = 70%), lunate sulcus (M = 80%; F = 60%), lateral calcarine (M = 30%; F = 10%), superior temporal sulcus (M = 80%; F = 100%), rhinal sulcus (M = 50%; F = 70%), occipitotemporal sulcus (M = 30%; F = 60%) and ascending ramus (M = 30%; F = 10%). We noted sex differences in the LHs in the impression of the precentral sulcus (M = 20%; F = 50%), postcentral sulcus (M = 30%; F = 10%), intraparietal sulcus (M = 40%; F = 20%), transverse occipital

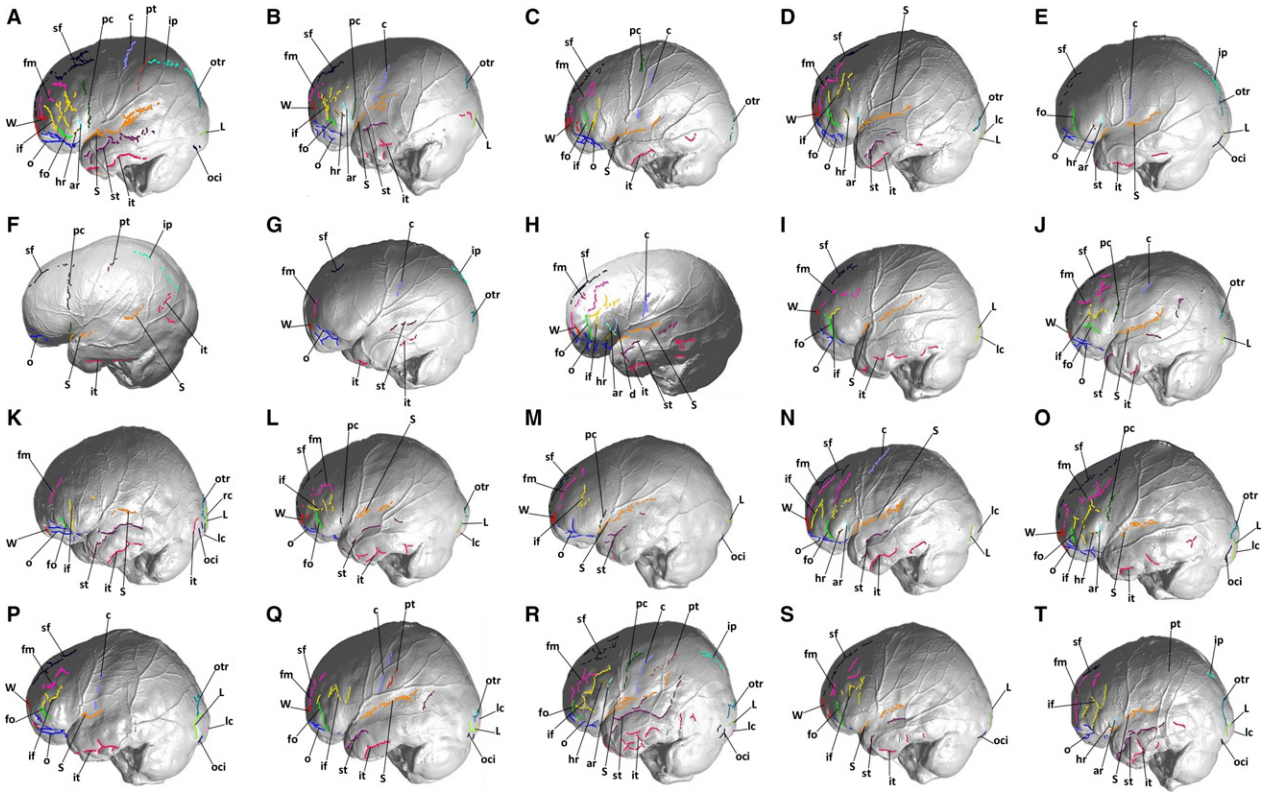

Fig. 2 Sulcal imprints observed on the left hemisphere of 20 individuals. ar = ascending ramus, c = central, d = diagonal, W = fronto-marginal, fo = fronto-orbital, hr = anterior horizontal ramus, if = inferior frontal, ip = intraparietal, it = inferior temporal, L = Lunate, lc = lateral calcarine, fm = middle frontal, o = orbital, oci = inferior/lateral occipital, otr = transverse occipital, pc = precentral, pt = postcentral, rc = retro-calcarine, S = Sylvian fissure, sf = superior frontal, st = superior temporal.

(M = 60%; F = 80%), lunate sulcus (M = 70%; F = 90%), retro-calcarine sulcus (M = 30%; F = 10%), anterior horizontal ramus (M = 30%; F = 50%) and ascending ramus (M = 30%; F = 50%).

Discussion

Sulci identification

In this study, we used high-definition X-ray microtomography to explore variation in sulcal patterns in 20 extant human endocasts. With this method, we could reliably identify the orbital, temporal and frontal sulci and the Sylvian fissure in more than 80% of the endocasts. Descriptions of frequency and configuration of the orbital sulci, fronto-marginal, fronto-orbital and lateral occipital sulci are consistent with previous descriptions of brain sulci (Ono et al. 1990; Chiavaras & Petrides, 2000; Iaria & Petrides, 2007). We were able to identify both the fronto-marginal and fronto-orbital sulci on the endocasts, despite identification of these features in humans being a rather controversial topic (see Connolly, 1950; Petrides et al. 2012; Falk et al. 2018).

We could identify the precentral sulcus in fewer than half of the individuals; this may be due to distortion by the anterior bregmatic branch of the middle meningeal vessels (Bruner et al. 2018). Similarly, we could not reliably identify the postcentral sulcus, which may be due to the complex branching networks of blood vessels covering this area. Cerebrospinal fluid and blood vessels usually fill the main sulci delineated functional areas and may not reproduce well on endocasts (Zollikofer & León, 2013). Additionally, the transverse occipital sulcus can easily be misidentified on endocasts due to the tendency of the intraparietal sulcus to terminate posteriorly close to the lambdoid suture, which frequently creates phantom markings on the endocast.

Various morphological and functional differences have been noted between male and female brains (Holloway & de Lacoste, 1986; Zilles et al. 2001; Liu et al. 2010; Glezerman, 2016). Although morphological differences may exist between male and female brains, these differences may not extend to sulcal patterns or sulcal imprint visibility (this study). We noted significant asymmetry between the left and right hemispheres when identifying the lateral calcarine sulcus, rhinal sulcus and collateral sulcus. The rhinal and collateral sulcal imprints are frequently misidentified on endocasts due to their vulnerability to distortion imposed by localised bony elements, which may also explain the perceived asymmetry. The lateral calcarine

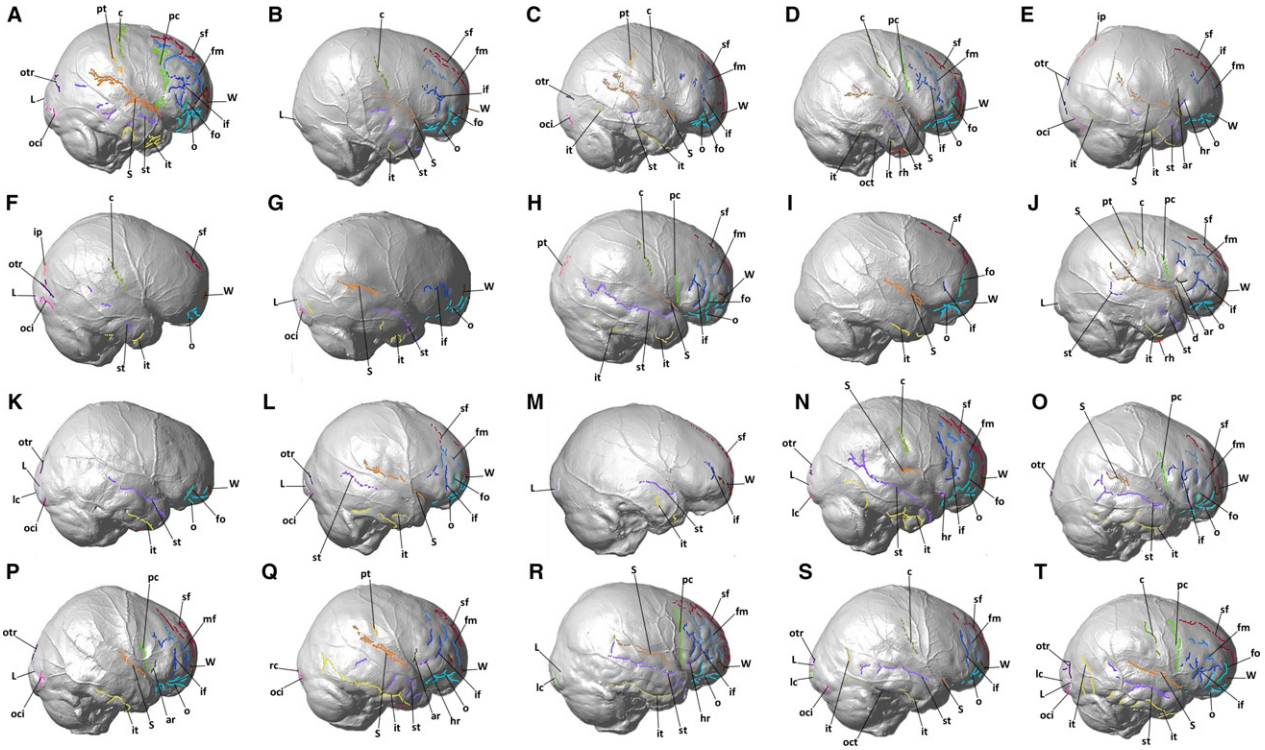

Fig. 3 Sulcal imprints observed on the right hemisphere of 20 individuals. ar = ascending ramus, c = central, d = diagonal, W = frontomarginal, fo = fronto-orbital, hr = anterior horizontal ramus, if = inferior frontal, ip = intraparietal, it = inferior temporal, L = Lunate, lc = lateral calcarine, fm = middle frontal, o = orbital, oci=inferior/lateral occipital, oct = occipitotemporal, otr = transverse occipital, pc = precentral, pt = postcentral, rc = retro-calcarine, rh = rhinal, S = Sylvian fissure, sf = superior frontal, st = superior temporal.

sulcus may also be asymmetrical (LHs = 55%; RHs = 20%), due to distortion occasionally created by overlay of the right dominant dural venous sinus groove (García-Tabernero et al. 2018).

Minh & Hamada (2017) found that the expression of sulcal imprints on endocasts of Japanese macaques decreased with age, and other studies have proposed that no new brain expansion occurs in older individuals (Liu et al. 2010), making it harder to identify sulcal imprints in crania of older individuals. We excluded age as a variable due to sample size constraints.

Implications for palaeoneurological studies

We identified sulci delimiting crucial cortical areas in the brain in more than one-third of the crania, including the lunate sulcus and the anterior horizontal and ascending rami of the Sylvian fissure, which are involved in critical debates in human palaeoneurology (Sherwood et al. 2008; Falk, 2014). In particular, frontal sulci delimit crucial functional areas in neuroscience, including language, memory and motor functions (Petrides, 2005; Petrides et al. 2012). The horizontal and the ascending rami of the Sylvian fissure, which we identified in nearly half of the samples on the LH, have been suggested to have emerged with the genus *Homo*, but the recent discovery of a non-human

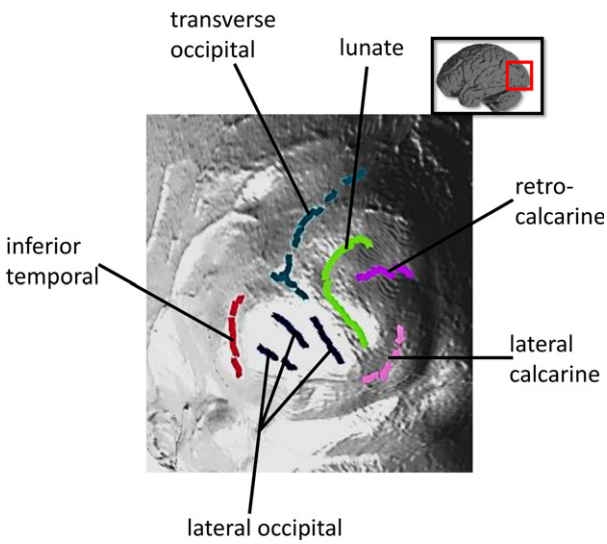

Fig. 4 Occipital view showing the lunate sulcus impression in one selected individual.

hominin endocast with an intermediate pattern between the ape-like and human-like patterns suggests a more complex scenario (Falk, 1983; Tobias, 1987; Carlson et al. 2011; but see discussion in Falk et al. 2018) . The middle frontal sulcus is also of particular interest in palaeoneurology due

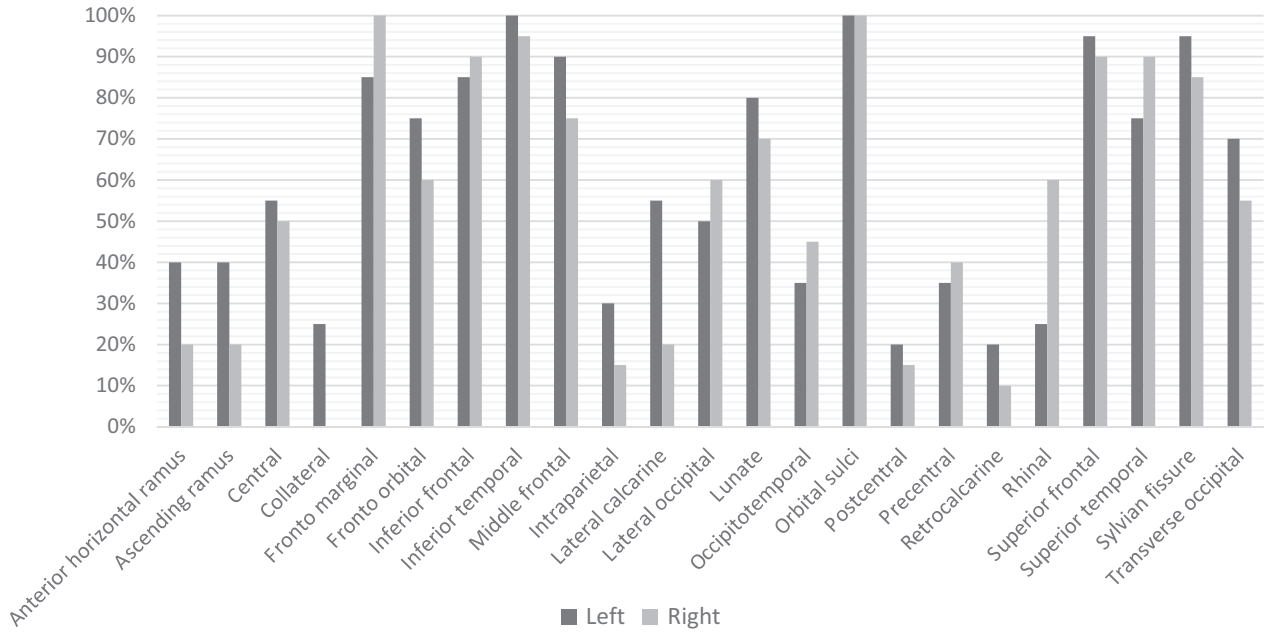

Fig. 5 Frequency of sulci observed in the left and right hemispheres of human endocasts.

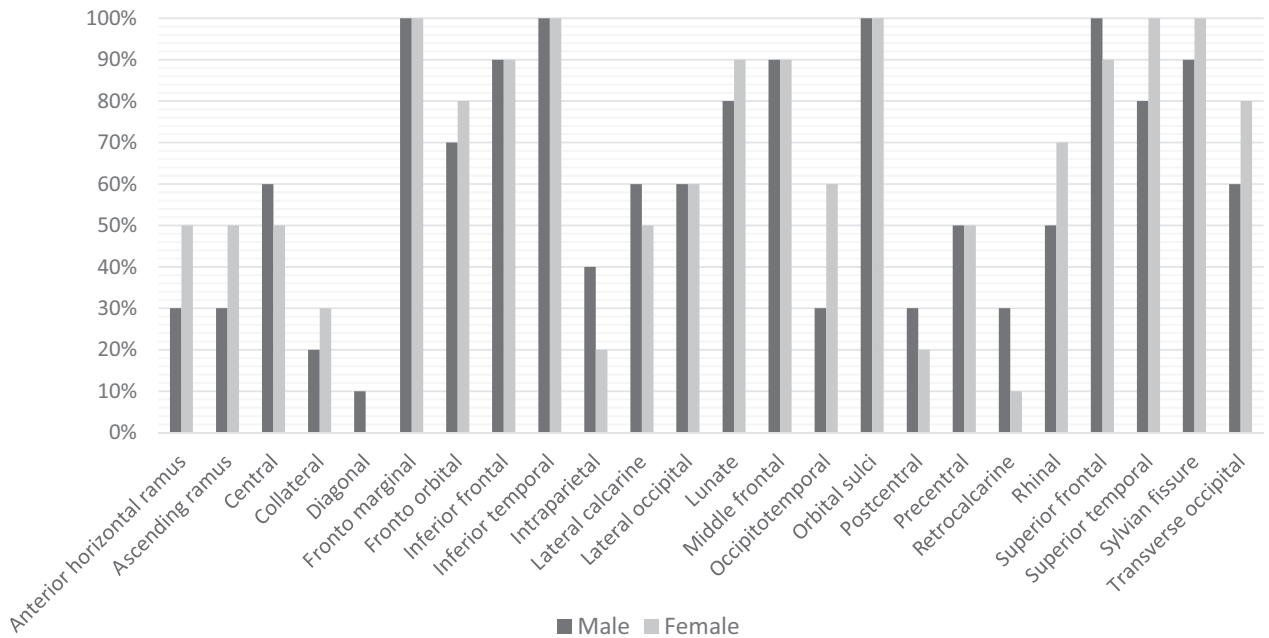

Fig. 6 Frequency of sulci observed in male and female human endocasts.

to its presence in non-human hominin endocasts and its relationship to the dorsolateral prefrontal cortex, which is involved in executive functions (Connolly, 1950; Van Essen, 2007; Falk, 2014). From a comparative perspective, the rostral part of the middle frontal sulcus is considered to be a homologue of the sulcus rectus in monkeys, whereas the caudal part is unique to humans, and is associated with the expansion of the frontal lobe (Eberstaller, 1890; Connolly, 1950; Falk, 2014).

The lunate sulcus has been extensively described in association with human brains and is highly variable (Smith, 1903; Connolly, 1950; Ono et al. 1990; Duvernoy et al. 1999; Holloway et al. 2004; Allen et al. 2006). Although our sample size was small, the lunate sulcus was observed in 75% of the crania, which is more than the 62% in Ono et al. (1990) and 51.8% in Allen et al. (2006). Larger sample sizes (studied using similar methods or other populations) could shed more light on this matter. We observed the lunate sulcus

anterior to the caudal pole of the occipital lobe as fragmented, vertically orientated impressions, usually depicting a curve (Fig. 4). In one case we could visualise a lunate sulcus as described by Allen et al. (2006), traversing a substantial portion of the lateral surface of the posterior portion of the occipital lobe. As observations were made on endocasts and not cerebral surfaces, we are not able to comment on whether this impression is made by a 'true' or a composite lunate sulcus; however, humans generally do not have 'true' lunate sulci (Connolly, 1950; Allen et al. 2006; Alves et al. 2012). Nevertheless, our ability to detect the lunate sulcus (or, at the very least, fragments thereof) is important due to the past and ongoing debate regarding the homology of the lunate sulcus in humans and apes, and the identification of the lunate sulcus in early hominin endocasts (Falk, 1980b, 2014; Holloway, 1981). The caudal placement of the lunate sulcus in hominins older than 2 million years may indicate early changes in the occipital lobes, probably related to the expansion of the parietal association cortex and a mosaic evolution of the cerebral areas (Falk, 1980b, 2014; Holloway, 1981, 2001).

We were also able to identify the lateral calcarine sulcus more often than previously reported, namely in half of the crania (see Connolly, 1950), whereas Alves et al. (2012) identified a calcarine fissure on the superolateral surface of the brain at the level of the lateral occipital sulcus in 40% of brains. The size of the calcarine sulcus and its association with the primary visual cortex has recently been discussed in Neanderthal brain endocasts, which revealed potential differences in visual capacity when compared with *Homo sapiens* (García-Tabernero et al. 2018).

In conclusion, our semi-automatic sulcal detection approach allowed us to identify sulci involved in crucial functions and long-standing debates in palaeoanthropology. Despite the automatic sulci detection applied in this study, the identification of sulci by human observers may represent a potential bias that should be taken into account when interpreting sulcal imprints in the fossil record. Accordingly, this atlas will subsequently be used to construct a statistical model documenting sulcal variation in extant humans and, ultimately, to develop a protocol for the automatic recognition of cerebral imprints in fossil hominin endocasts, which will aid investigations pertaining to cortical evolution in the fossil record (Beaudet, 2017).

Acknowledgements

We thank G. Krüger (University of Pretoria) for collection access; F. de Beer and L. Bam (Necsa, DST-NRF Grant number: UID 72310) for data acquisition; J. Dumoncel (AMIS–UMR5288) for technical support; Dr C. Tosh (University of Pretoria) for editorial assistance. E. de Jager is supported by the National Research Foundation of South Africa (Grant Number: 112186) and the Erasmus Mundus program 'A European and South African Partnership on Heritage and Past+' (AESOP+ program). A. Beaudet is funded by the Centre of Excellence in Palaeosciences, the Claude Leon Foundation and the French Institute of South Africa.

References

Allen JS, Bruss J, Damasio H (2006) Looking for the lunate sulcus: A magnetic resonance imaging study in modern humans. *Anat Rec* **288**, 867–876.

Alves RV, Ribas GC, Parraga RG, et al. (2012) The occipital lobe convexity sulci and gyri. *J Neurosurg* **116**, 1014–1023.

Amunts K, Schleicher A, Burgel U, et al. (1999) Broca's region revisited: cytoarchitecture and intersubject variability. *J Comp Neurol* **412**, 319–341.

Beaudet A (2017) The emergence of language in the hominin lineage: perspectives from fossil endocasts. *Front Hum Neurosci* **11**, 427.

Beaudet A, Gilissen E (2018) Fossil primate endocasts: perspectives from advanced imaging techniques. *In: Digital Endocasts*; pp. 47–58. Tokoyo: Springer.

Beaudet A, Dumoncel J, de Beer F, et al. (2016a) Morphoarchitectural variation in South African fossil cercopithecoid endocasts. *J Hum Evol* **101**, 65–78.

Beaudet A, Dumoncel J, de Beer F, et al. (2016b) Morphoarchitectural variation in the extant human endocast. In: *European Society for the Study of Human Evolution*. (eds Plavcan M, Elton S, Teaford M), p. 46. Madrid: Journal of Human Evolution.

Bruner E, Ogihara N (2018) Surfin' endocasts: The good and the bad on brain form. *Palaeontol Electron* **21**, 1–10.

Bruner E, Ogihara N, Tanabe HC (2018) *Digital Endocasts: from Skulls to Brains*. Tokoyo: Springer.

Carlson KJ, Stout D, Jashashvili T, et al. (2011) The endocast of MH1, *Australopithecus sediba*. *Science* **333**, 1402–1407.

Chiavaras MM, Petrides M (2000) Orbitofrontal sulci of the human and macaque monkey brain. *J Comp Neurol* **422**, 35–54.

Connolly CJ (1950) *External morphology of the primate brain*. Springfield, IL: CC Thomas.

Duvernoy H, Bourgouin P, Cabanis E, et al. (1999) *The Human Brain: Functional Anatomy, Vascularization and Serial Sections with MRI*. New York: Springer.

Eberstaller O. (1890) Das Stirnhirn. Munich: Urban & Schwarzenberg.

Falk D (1980a) Comparative study of the endocranial casts of New and Old World monkeys. In: *Evolutionary Biology of the New World Monkeys and Continental Drift*. (eds Chiochon RL, Chiarelli AB), pp. 275–292. Boston: Springer.

Falk D (1980b) A reanalysis of the South African australopithecine natural endocasts. *Am J Phys Anthropol* **53**, 525–539.

Falk D (1983) Cerebral Cortices of East African Early Hominids. *Science* **221**, 1072–1074.

Falk D (2014) Interpreting sulci on hominin endocasts: old hypotheses and new findings. *Front Hum Neurosci* **8**, 134.

Falk D, Zollikofer CPE, Ponce de Leon M, et al. (2018) Identification of in vivo Sulci on the external surface of eight adult chimpanzee brains: implications for interpreting early hominin endocasts. *Brain Behav Evol* **91**, 45–58.

Fischl B, Rajendran N, Busa E, et al. (2008) Cortical folding patterns and predicting cytoarchitecture. *Cereb Cortex* **18**, 1973–1980.

García-Tabernero A, Peña-Melián A, Rosas A (2018) Primary visual cortex in neandertals as revealed from the occipital

remains from the El Sidrón site, with emphasis on the new SD-2300 specimen. *J Anat* **233**, 33–45.

Glezerman M (2016) Yes, there is a female and a male brain: Morphology versus functionality. *Proc Natl Acad Sci U S A* **113**, E1971.

Gunz P, Neubauer S, Maureille B, et al. (2010) Brain development after birth differs between Neanderthals and modern humans. *Curr Biol* **20**, R921–R922.

Hoffman JW, De Beer F. (2012) Characteristics of the micro-focus x-ray tomography facility (MIXRAD) at Necsa in South Africa. 18th World Conference on Nondestructive Testing; pp. 16–20.

Holloway RL (1978) The relevance of endocasts for studying primate brain evolution. *Sens Syst Primates*. Springer 181–200.

Holloway RL (1981) Revisiting the South African Taung australopithecine endocast: The position of the lunate sulcus as determined by the stereoplotting technique. *Am J Phys Anthropol* **56**, 43–58.

Holloway RL (2001) Does allometry mask important brain structure residuals relevant to species-specific behavioral evolution? *Behav Brain Sci* **24**, 286–287.

Holloway RL, de Lacoste MC (1986) Sexual dimorphism in the human corpus callosum: an extension and replication study. *Human Neurobiol* **5**, 87–91.

Holloway RL, Broadfield DC, Yuan MS (2004) *The Human Fossil Record*. Hoboken, NJ: John Wiley & Sons Inc.

Holloway RL, Hurst SD, Garvin HM, et al. (2018) Endocast morphology of *Homo naledi* from the Dinaledi Chamber, South Africa. *Proc Natl Acad Sci U S A* **22**, 5738–5743.

Iaria G, Petrides M (2007) Occipital sulci of the human brain: variability and probability maps. *J Comp Neurol* **501**, 243–259.

Kobayashi Y, Matsui T, Haizuka Y, et al. (2014) Cerebral sulci and gyri observed on Macaque endocasts. In: *Dynamics of Learning in Neanderthals and Modern Humans Volume 2: Cognitive and Physical Perspectives*; pp. 131–137 (eds Akazawa T, Ogihara N, C Tanabe H, et al.). Tokyo: Springer Japan.

L'Abbé EN, Loots M, Meiring JH (2005) The Pretoria bone collection: a modern South African skeletal sample. *HOMO* **56**, 197–205.

Le Gros Clark WE, Cooper DM, Zuckerman S (1936) The endocranial cast of the chimpanzee. *J R Anthropol Inst* **66**, 249–268.

Liu T, Wen W, Zhu W, et al. (2010) The effects of age and sex on cortical sulci in the elderly. *NeuroImage* **51**, 19–27.

Minh N, Hamada Y (2017) Age-related changes of sulcal imprints on the endocranium in the Japanese macaque *Macaca fuscata*. *Am J Phys Anthropol* **163**, 285–294.

Neubauer S (2014) Endocasts: possibilities and limitations for the interpretation of human brain evolution. *Brain Behav Evol* **84**, 117–134.

Neubauer S, Gunz P, Weber GW, et al. (2012) Endocranial volume of *Australopithecus africanus*: new CT-based estimates and the effects of missing data and small sample size. *J Hum Evol* **62**, 498–510.

Neubauer S, Gunz P, Leakey L, et al. (2018) Reconstruction, endocranial form and taxonomic affinity of the early *Homo calvaria* KNM-ER 42700. *J Hum Evol* **121**, 25–39.

Ono M, Kubik S, Abernathey CD (1990) *Atlas of the Cerebral Sulci*. Stuttgart: Georg Thieme Verlag.

Petrides M (2005) Lateral prefrontal cortex: architectonic and functional organization. *Philos Trans R Soc Lond B Biol Sci* **360**, 781–795.

Petrides M, Pandya DN. ((2012) Chapter 26 - The frontal cortex A2. In: *The Human Nervous System*. (ed. Paxinos G), Third ed, pp. 988–1011. San Diego: Academic Press.

Ribas GC (2010) The cerebral sulci and gyri. *Neurosurg Focus* **28**, E2.

Sherwood CC, Subiaul F, Zawidzki TW (2008) A natural history of the human mind: tracing evolutionary changes in brain and cognition. *J Anat* **212**, 426–454.

Smith GE (1903) The so-called affenspalte in the human (Egyptian) brain. *Anat Anz* **24**, 74–83.

de Sousa A, Cunha E (2012) Hominins and the emergence of the modern human brain. In: *Progress in Brain Research: Evolution of the Primate Brain* (eds Hofman MA, Falk D), pp. 293–322. London: Elsevier.

Spoor F, Jeffery N, Zonneveld F (2000) Using diagnostic radiology in human evolutionary studies. *J Anat* **197**, 61–76.

Subsol G, Thirion J-P, Ayache N (1996) Construction automatique d'atlas anatomiques morphométriques à partir d'images médicales tridimensionnelles: application à un atlas du crâne. *Trait Signal* **13**, 651–674.

Subsol G, Thirion J-P, Ayache N (1998) A scheme for automatically building three-dimensional morphometric anatomical atlases: application to a skull atlas. *Med Image Anal* **2**, 37–60.

Subsol G, Gesquiere G, Braga J, et al. (2010) 3D automatic methods to segment' virtual' endocasts: state of the art and future directions. *Am J Phys Anthropol*. 141(suppl. 50), 226-227 (abstract).

Tobias PV (1987) The brain of *Homo habilis*: A new level of organization in cerebral evolution. *J Hum Evol* **16**, 741–761.

Van Essen D (2007) Cerebral cortical folding patterns in primates: why they vary and what they signify. In: *Evolution of Nervous Systems* (eds Kaas J, Preuss T), pp. 267–276. London: Elsevier.

Yoshizawa S, Belyaev A, Yokota H, et al. (2007) Fast and faithful geometric algorithm for detecting crest lines on meshes. 15th Pacific Conference on Computer Graphics and Applications. IEEE, 231–237.

Yoshizawa S, Belyaev A, Yokota H, et al. (2008) Fast, robust, and faithful methods for detecting crest lines on meshes. *Comput Aided Geom Des* **25**, 545–560.

Zilles K, Kawashima R, Dabringhaus A, et al. (2001) Hemispheric shape of European and Japanese brains: 3-D MRI analysis of intersubject variability, ethnical, and gender differences. *NeuroImage* **13**, 262–271.

Zollikofer CPE, León MSP (2013) Pandora's growing box: inferring the evolution and development of hominin brains from endocasts. *Evol Anthropol* **22**, 20–33.